ELSEVIER

Journal of Nuclear Materials 258–263 (1998) 1606–1612

journal of nuclear materials

Flux and composition dependence of irradiation creep of austenitic alloys irradiated in PFR at ~420°C

M.B. Toloczko [a,*], F.A. Garner [b], J. Standring [c], B. Munro [d], S. Adaway [d]

[a] *Washington State University, Pullman, WA 99163, USA*
[b] *Pacific Northwest National Laboratory, Richland, WA 99352, USA*
[c] *UKAEA, Harwell, UK*
[d] *AEA Technology, Dounreay, Scotland, UK*

Abstract

Swelling and irradiation creep of five austenitic stainless steel alloys irradiated at ~420°C in the Prototypic Fast Reactor (PFR) were examined. The specimens were in the form of pressurized creep tubes, constructed in the USA and irradiated in PFR in a joint USA/UK experiment. The alloy compositions varied greatly, with the greatest elemental variation in the nickel content, which ranged from 15% to 40% over the five alloys. For each alloy, at least two identical sets of tubes were constructed. Each tube-set was irradiated at a different neutron flux level. Swelling was observed to vary with both alloy composition and flux. Irradiation creep was examined from the perspective of the $\overline{B} = \dot{\bar{\varepsilon}}/\overline{\sigma} = B_0 + D\dot{S}$ creep model. The values of both creep coefficients, B_0 and D, were typical for austenitic stainless steels and were found to be insensitive to flux over the range of fluxes in this experiment. However, the creep coefficients may be mildly sensitive to alloy composition.

1. Introduction

In a continuing effort to better understand the factors which affect irradiation creep, previously unanalyzed data obtained from creep experiments performed many years earlier in the Prototypic Fast Reactor (PFR) were examined in this paper. These data offer the rare opportunity to study the effect of neutron flux on irradiation creep, providing insights which are useful in extrapolating existing irradiation creep data to a fusion-relevant environment. Several other researchers have studied the effect of neutron flux on irradiation creep and have shown a non-linear dependence of irradiation creep rate on neutron flux [1–3]. However, in a recent reexamination of a subset of Lewthwaite and coworkers data on the effect of neutron flux on irradiation creep [1] by Garner and Toloczko [4,5], it was concluded that the apparent dependence of the creep compliance, B_0, on neutron flux was due to the inadvertent inclusion of the irradiation creep transient, and that B_0 was largely independent of neutron flux.

In addition to flux variations, the effect of compositional variations on irradiation creep was also examined in this experiment using five austenitic stainless steels. These steels spanned a large range of nickel contents (15–40%) and also contained significant variations in most of the other alloying elements.

2. Experimental details

In PFR, the Demountable Subassembly (DMSA) irradiation vehicle was utilized and is described in detail in Ref. [6]. This vehicle is essentially a heat pipe, and specimens are located at various axial positions in and near the reactor core. Tube-sets placed near the core center experienced higher fluxes. [1] Temperature control

* Corresponding author. Present address: Battelle PNNL, MS P8-15, P.O. Box 999, Richland, WA 99352, USA. Tel.: +1 509 376 0156; fax: +1 509 376 0418; e-mail: mic@wsunix.wsu.edu.

[1] The original intent of this procedure was to supply several dose levels in one irradiation cycle. However, this procedure ignores the possible effect of flux on swelling, and this flux effect does not always allow data produced at different flux levels to be combined and analyzed as if they were flux-independent.

0022-3115/98/$19.00
PII: S0022-3115(98)00158-5

Table 1
Alloy compositions and heat treatments

Alloy	Heat	Ni	Cr	Mn	Mo	Si	C	Ti	Al	Zr	V	Cu	Nb
316 [a]	81 600	13.7	17.4	1.77	2.34	0.57	0.047	–	–	–	0.02	0.01	–
D9 [a]	2966	15.7	14.0	2.48	1.52	1.03	0.047	0.23	–	–	–	–	–
D21 [a]	K192	25.6	8.4	1.01	0.91	0.25	0.062	3.11	1.58	0.037	–	–	–
D68 [b]	K174	33.9	12.5	0.23	–	0.41	0.036	1.63	0.25	<0.01	–	–	2.79
D66 [c]	K171	40.2	11.1	0.21	1.98	0.48	0.040	3.01	1.48	0.049	–	–	–

[a] 20% CW.
[b] 25% CW.
[c] 25% CW + 800°C/2 h/AC + 700°C/2 h/AC.

in this vehicle was passive. Thermocouples were placed at the coolant inlet and outlet to the vehicle, and the reported temperature was the dose-weighted average of these inlet and outlet temperatures. The coolant inlet and outlet temperatures were not available to the authors for analysis, and without these details, it was not possible to estimate uncertainties in the specimen temperatures. Thus, it is possible that in addition to flux variations, small temperature variations may have also existed between tube-sets placed at widely separated positions along the heat pipe.

Helium pressurized tubes with 4.57 mm diameter and 0.203 mm wall thickness were constructed from the alloys with heat treatments and compositions described in Table 1. Tubes in each tube-set were pressurized to have hoop stresses ranging from 0 to 150 MPa when at the target irradiation temperature. Depending on the alloy, four to eight pressurized tubes comprised a tube-set.

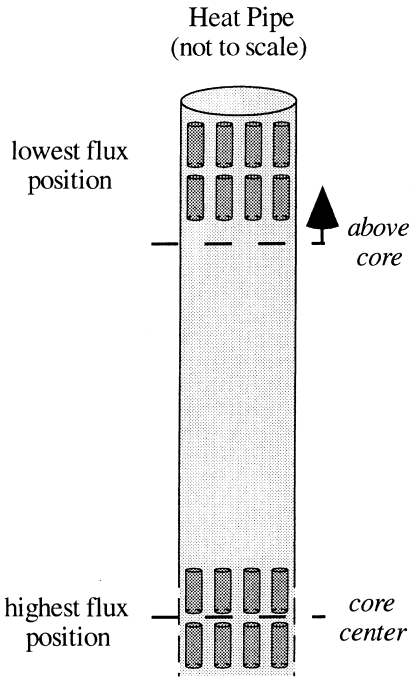

Fig. 1. Schematic of tube locations in the DMSA heat pipe.

Flux variations were achieved by placing two or more identical tube-sets at selected heights in the heat pipe. A schematic showing the basic placement of the tube-sets in the heat pipe is shown in Fig. 1. Volume constraints in the DMSA allowed only four tubes at a given reactor axial level, and tube-sets comprised of more than four tubes were divided between two adjacent axial locations, as depicted in Fig. 1. Although the tube subsets are adjacent, the difference in position results only in small flux variations and probably very small temperature differences. Absolute dose rates were not available for this report, but relative dose rates were calculated from the reported doses and are listed in Table 2.

Swelling and creep strains were calculated from diameter measurements of the tubes. These measurements are performed using a laser profilometry technique that is described elsewhere [7]. The accuracy of the measurement technique is within ±0.5 μm. However, diameter variations along the tube are greater than the measurement accuracy. Typical diameter variations fall within ±10 μm. For the 4.57 mm (4570 μm) diameter pressurized tubes used in this study, the error in the diameter measurement is less than ±0.5% of the measurement.

After irradiation and measurement, tubes were returned to the reactor for further irradiation and subsequent measurement. Two irradiation cycles were completed for this experiment. The highest total dose was about 50 dpa. Reported doses are given in dpa for iron which varies only a few percent from the actual dpa for the range of alloy compositions studied.

Swelling was estimated from diameter measurement of the stress-free tube in each tube-set. This is not an optimal method for swelling measurement because any stress-enhanced swelling that may have occurred in a stressed tube is not measured. With the stress-free swelling estimate, irradiation creep can be estimated by removing the linear "swelling strain" from the total diametral strain measured in a stressed tube.

Table 2
Summary of creep coefficients for the alloys examined in this work

Alloy	wt% Ni	$B_0 \times 10^{-6}$ MPa^{-1} dpa^{-1}			$D \times 10^{-2}$ MPa^{-1}			ϕ/ϕ_{max}		
		Tube-set 1	Tube-set 2	Tube-set 3	Tube-set 1	Tube-set 2	Tube-set 3	Tube-set 1	Tube-set 2	Tube-set 3
316 SS	14	– [a]	1.58	2.63	–	0.59	0.19	–	~0.65	1.0
D9	16	–	1.14	1.00	–	1.54	1.62	–	~0.85	1.0
D21	26	–	1.37	1.39	–	1.30	1.40	–	~0.30	1.0
D68	34	–	0.85	1.12	–	1.32	1.24	–	~0.50	1.0
D66	40	1.12	0.67	1.14	0.36	0.33	0.50	~0.25	~0.40	1.0

[a] Only two flux levels for 316 SS, D9, D21, and D68.

3. Results

3.1. Swelling observations

For some of the alloys examined, precipitate-related densification was observed as negative diametral strains. This often-observed phenomenon is attributed to phase-related changes in the matrix composition of the alloy [8–10]. Densification observed in the swelling measurements of the D66 unstressed tubes is shown in the top part of Fig. 2. Assuming densification is independent of stress, subtracting the fractional diameter change of the stress-free tube from the fractional diameter change of a stressed tube removes both swelling and any densification from the total strains of the stressed tube.

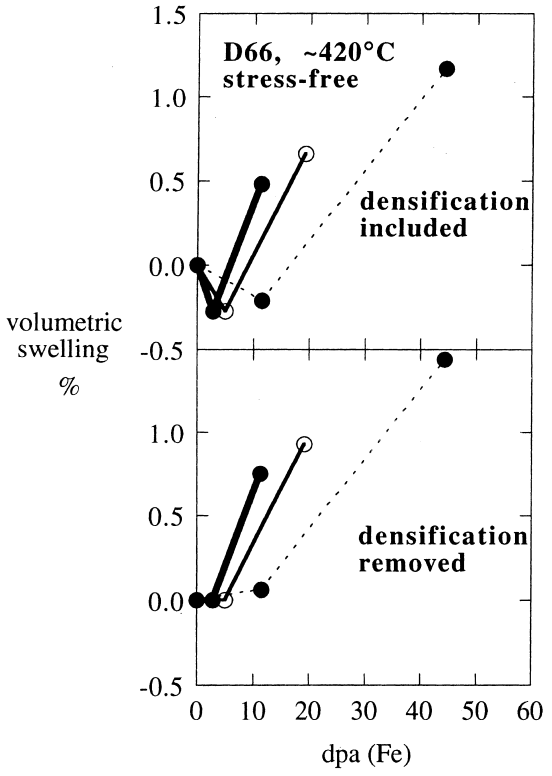

Fig. 2. Densification and flux-affected swelling incubation period observed in D66 stress-free tubes.

Removing the densification-related contractions from the swelling estimate of a stress-free tube presents more difficulty, however. There is no accurate method for distinguishing densification-related diameter changes from swelling-related diameter changes when both mechanisms are acting. The method adopted here has been to assume that the amount of phase-related densification which occurs is equal to the observed densification of the stress-free tube after the first irradiation cycle. This assumes densification is flux-independent over the range of neutron fluxes in this experiment. This value was then subtracted from all the later diameter measurements at higher dpa levels. Where stress-free tubes of the same alloy were placed at different positions along the pipe to achieve variations in flux, the largest densification that occurred among the stress-free tubes was the value assigned to the densification of all the stress-free tubes of that alloy. The lower part of Fig. 2 shows the densification removed from the D66 stress-free tubes using this method. The estimated volumetric densification observed in the stress-free tubes of each of the alloys after the first irradiation cycle, assuming isotropic densification, is reported in Table 3.

Fig. 3 shows the observed swelling, with densification removed, of all five alloys. Alloy 316 swelled the most while the D21 alloy swelled the least. The swelling sensitivity to flux and small temperature differences was

Table 3
Densification observed in stress-free tubes after the first irradiation cycle

Alloy	Volumetric contraction, %		
	Tube-set 1	Tube-set 2	Tube-set 3
316	– [a]	None	−0.03
D9	–	−0.24	−0.21
D21	–	−0.29	−0.32
D68	–	−0.54	−0.57
D66	−0.27	−0.27	−0.21

[a] Only two flux levels for 316 SS, D9, D21, and D68.

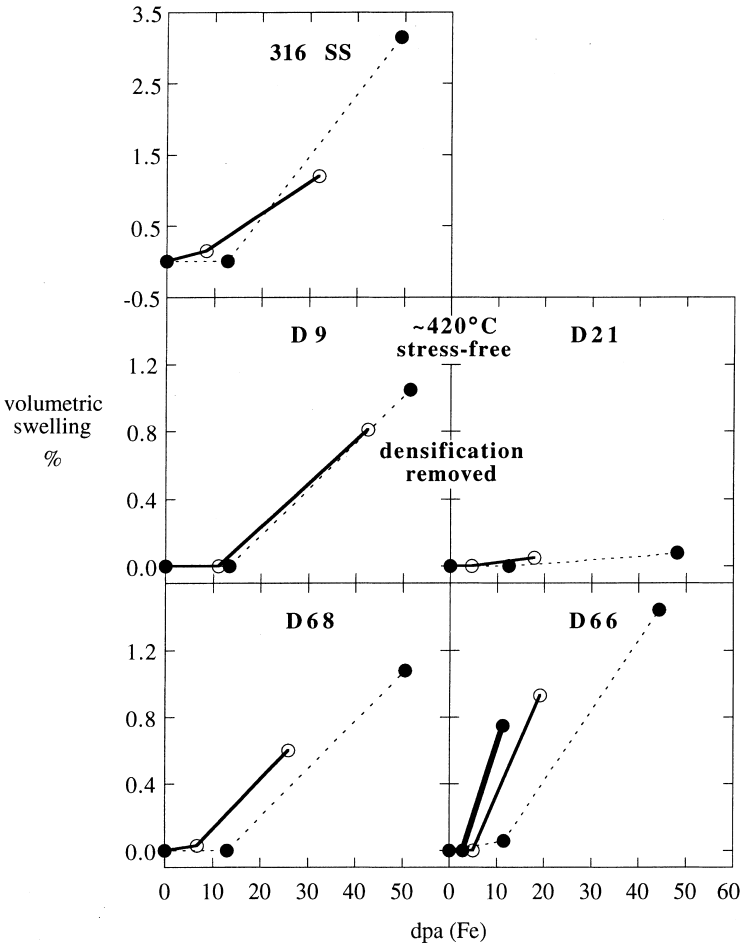

Fig. 3. Swelling versus dose. Note different volumetric swelling scale for 316 SS.

varied, with the D9 showing virtually no sensitivity and D68 and D66 showing significant sensitivity. It is not surprising that D9 showed little flux sensitivity as the lower flux tube-set ran at about 85% of the flux of the higher flux tube-set. The observed sensitivity was marked by reduced incubation periods at lower fluxes. Post-transient swelling rates do not appear to be strongly affected by the range of flux variations studied.

3.2. Irradiation creep strains

The midwall creep strains plotted versus dose are shown in Fig. 4. There is not much difference in irradiation creep behavior between the low and high flux tube-sets. With the exception of the 316 SS, the relative magnitude of the irradiation creep strains mirror the relative magnitudes of the observed swelling in the various alloys.

Shown in Fig. 5 are the midwall creep strains plotted versus stress. The open and closed symbols indicate the tubes in a tube-set that were located in vertically adjacent positions in the heat pipe. As mentioned previously, these small differences in axial position resulted in small dose differences as shown in the figure. In all cases, the irradiation creep strains at a given dpa level were linear with stress over the range of stresses studied.

4. Discussion

As mentioned in the introduction, the two main objectives of this work were to examine the effect of flux and composition on irradiation creep. The influence of flux and composition were examined in the framework of the familiar $\overline{B} = \dot{\bar{\varepsilon}}/\overline{\sigma} = B_0 + D\dot{S}$ creep model, where $\dot{\bar{\varepsilon}}$ is the effective (i.e. von Mises) creep rate, $\overline{\sigma}$ is the effective stress, B_0 is the creep compliance, D is the creep-swelling coupling coefficient, and $\dot{S}$ is the volumetric swelling rate. B_0 is the stress-normalized creep rate that occurs in absence of swelling, and $D\dot{S}$ represents an

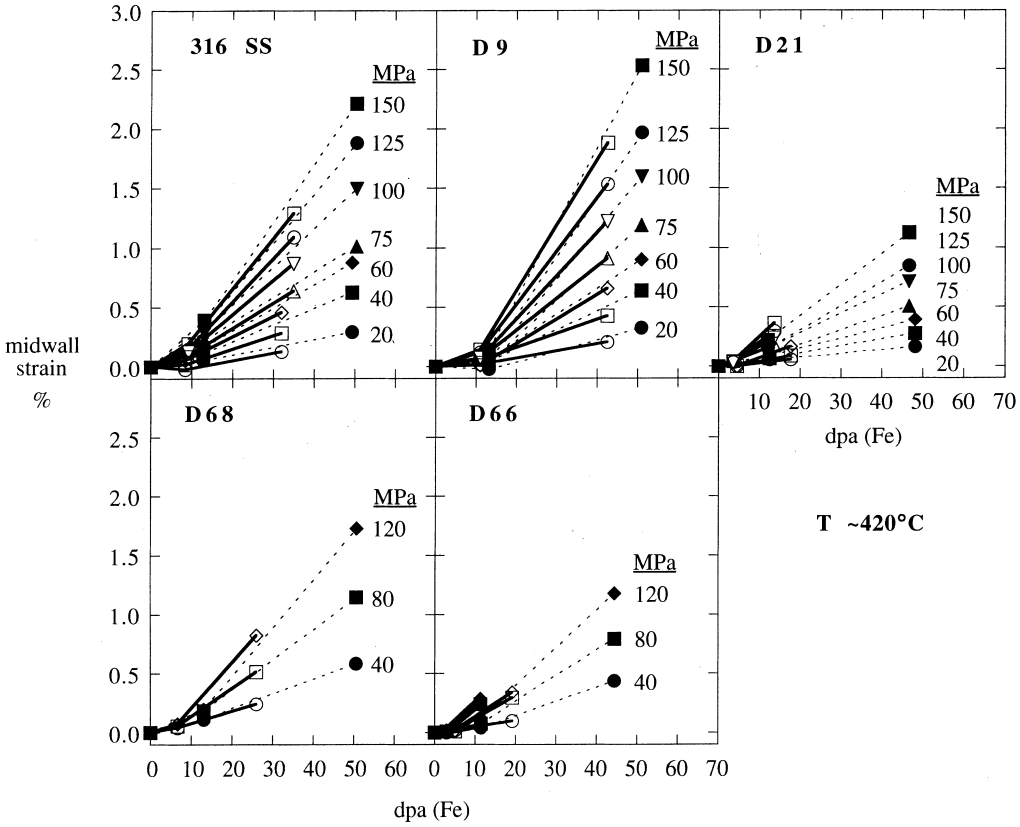

Fig. 4. Midwall creep strains versus dose.

addition to the stress-normalized creep rate that occurs when the material swells. There are some limitations to the application of this model, however. The model assumes that B_0 and D are constants, but recent experimental work [10,11] and theory [12] suggest that D is not really a constant. It has been shown that stress-enhanced swelling masks the decline in the magnitude of D as the swelling rate increases.

The interpretation of this experiment is somewhat limited in that only stress-free swelling measurements were available, and it has been shown that swelling in both austenitic and ferritic steels is enhanced by an applied stress [13–15]. The creep coefficients, B_0 and D, were calculated for each tube-set based on stress-free swelling and are summarized in Table 2.

The calculated values for B_0 are typical for 316 SS and D9 irradiated in the 400–450°C temperature range [16–19], and it appears these values are largely independent of flux but show some apparent compositional dependence which is thought to reflect our inability to completely separate the creep and densification strains. The flux independence of B_0 agrees with Garner and Toloczko's reinterpretation [4,5] of Lewthwaite and Mosedale's study of irradiation creep in cold-worked FCC steels [1]. However, Grossbeck et al. [3] had earlier compiled most of the other work on the neutron flux dependence of irradiation creep, and this compilation supports a square root dependence of irradiation creep rate on neutron flux. It is suspected by the authors of this paper that transient effects also dominated the other experiments reviewed by Grossbeck.

In the current study, values of the creep-swelling coupling coefficient, D, are somewhat more variable but also appear to be largely independent of neutron flux. Composition appears to have a marked effect on D in the case of the 316 SS and the D66 alloy. The variation in D is difficult to associate with any particular compositional variation because the concentration of many solutes was varied between these alloys. The variation in D-coefficient may also arise, in part, from the compositional sensitivity of stress-enhanced swelling. The range of D-coefficients overlaps with the range observed in prior studies of 316 type steels [16,17,20].

The relative flux-independence of the creep coefficients suggest that the irradiation creep strains in Fig. 4 ought to mirror the flux-dependent swelling behavior shown in Fig. 3, and indeed, such behavior can be observed in the 316 SS, the D21, and in some of the D66

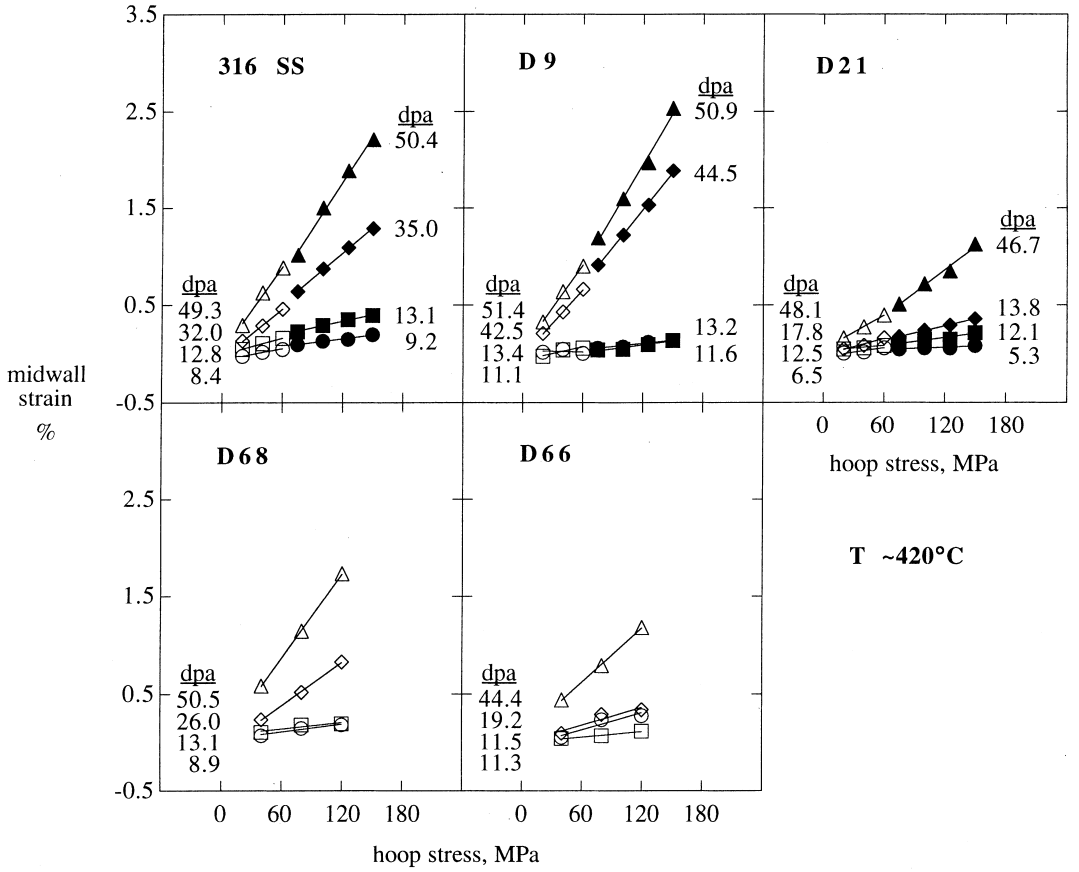

Fig. 5. Midwall creep strains versus hoop stress.

pressurized tubes. In the other alloys, the mirroring behavior is not so clear. The reason may lie in the small differences in the creep coefficients which likely arise from experimental uncertainties and the inability to accurately separate all the mechanisms contributing to the diameter change of the creep tubes.

5. Conclusions

Five austenitic stainless steels, in the form of pressurized creep tubes, were irradiated in PFR at ~420°C at several dose rates simultaneously. The alloy compositions varied greatly, with the greatest elemental variation in the nickel content, which ranged from 15% to 40%. Swelling of the stress-free pressurized tubes was observed to vary with both flux (and possibly temperature) as well as composition. Irradiation creep was linear with stress, and the creep compliance, B_0, was observed to be relatively independent of both composition and flux, whereas the creep-swelling coupling coefficient, D, was observed to be independent of flux but possibly somewhat dependent on composition. The derived values for B_0 and D were typical of earlier studies of austenitic stainless steels containing ~15% nickel [16–19].

References

[1] G.W. Lewthwaite, D. Mosedale, J. Nucl. Mater. 90 (1980) 205.
[2] G.W. Lewthwaite, D. Mosedale, in: Proceedings of the Conference on Dimensional Stability and Mechanical Behavior of Irradiated Metals and Alloys, vol. 1, BNES, 1983, pp. 129–132.
[3] M.L. Grossbeck, K. Ehrlich, C. Wassilew, J. Nucl. Mater. 174 (1990) 264.
[4] F.A. Garner, M.B. Toloczko, J. Nucl. Mater. 251 (1997) 252.
[5] F.A. Garner, M.B. Toloczko, S.I. Porollo, A.N. Vorobjev, A.M. Dvoriashin, Yu.V. Konobeev, in: The Eighth International Symposium on Effects of Degradation of Materials in Nuclear Power Systems – Water Reactors, 10–14 August 1997, Amelia Island, FL, 1987, pp. 834–845.
[6] C.L. Dodd et al., Paper 20, 28th Irradiation Devices Plenary Meeting, Brasimone, 1984.

[7] E.R. Gilbert, B.A. Chin, Effects of Radiation on Materials: Tenth Conference, ASTM STP 725, 1981, pp. 665–679.
[8] M.B. Toloczko, G.E. Lucas, G.R. Odette, R.E. Stoller, M.L. Hamilton, in: Seventeenth International Symposium on the Effect of Radiation on Materials, ASTM STP 1270, 1996, pp. 902–918.
[9] F.A. Garner, W.V. Cummings, J.F. Bates, E.R. Gilbert, HEDL-TME 78-9, June 1978.
[10] F.A. Garner, Materials Science and Technology, a Comprehensive Treatment, vol. 10a, VCH Publishers, Weinheim, 1994, p. 507.
[11] M.B. Toloczko, F.A. Garner, J. Nucl. Mater. 212–215 (1994) 509.
[12] C.H. Woo, F.A. Garner, J. Nucl. Mater. 191–194 (1992) 1309.
[13] F.A. Garner, E.R. Gilbert, D.L. Porter, Effects of Radiation on Materials: Tenth Conference, ASTM STP 725, 1981, pp. 680–697.
[14] T. Lauritzen, S. Vaidyanathan, W.L. Bell, W.J.S. Yang, Radiation Induced Changes in Microstructure: Thirteenth International Symposium (Part 1), ASTM STP 955, 1987, pp. 101–113.
[15] M.B. Toloczko, F.A. Garner, C.R. Eiholzer, J. Nucl. Mater. 212–215 (1994) 604.
[16] M.B. Toloczko, F.A. Garner, C.R. Eiholzer, J. Nucl. Mater. 191–194 (1992) 803.
[17] F.A. Garner, D.L. Porter, J. Nucl. Mater. 155–157 (1988) 1006.
[18] M.L. Grossbeck, L.K. Mansur, M.P. Tanaka, Effects of Irradiation on Materials: 14th International Symposium (vol. II), ASTM STP 1046, 1990, pp. 537–550.
[19] K. Herschbach, W. Schneider, K. Ehrlich, J. Nucl. Mater. 203 (1993) 233.
[20] V.S. Neustrov, V.K. Shamardin, Effects of Radiation on Materials: 16th International Symposium, ASTM STP 1175, 1993, pp. 816–823.